FINAL REPORT for GRANT NAGW-1848

TITLE: Observations of the Magnetopause Current Layer: Cases with No Boundary Layer and Tests of Recent Models

P.I. **Dr. Timothy E. Eastman**

Institution: University of Maryland

ph: 301–405–4829; email: eastman@glue.umd.edu

INDEX

INTRODUCTION

The magnetopause is the outer boundary of the Earth's magnetosphere, the region within which charged particle motion is dominated by the geomagnetic field. Adjoining the magnetopause, on its Earthward side, is usually found a boundary layer formed by plasmas of intermediate densities and temperatures which constitutes a transition layer from the shocked solar wind or magnetosheath plasmas to the field-dominated plasmas of the outer magnetosphere. Since the first direct and unique measurements of magnetospheric boundary layers (Rosenbauer et al., 1975; Eastman et al., 1976; Paschmann et al., 1976), boundary layers have been found to be present in about 90% of all magnetopause crossings.

Evidence for the probable existence of magnetospheric boundary layers was first presented by Hones et al. (1972) based on VELA satellite plasma observations (no magnetic field measurements were obtained). This magnetotail boundary layer is now known to be the tailward extension of the high-latitude boundary layer or plasma mantle (first uniquely identified using HEOS 2 plasma and field observations by Rosenbauer et al., 1975) and the low-latitude boundary layer (first uniquely identified using IMP 6 plasma and field observations by Eastman et al., 1976). The magnetospheric boundary layer is the region of magnetosheath-like plasma located Earthward of, but generally contiguous with the magnetopause. This boundary layer is typically identified by comparing low-energy (< 10 keV) ion spectra across the magnetopause. Low-energy electron measurements are also useful for identifiying the boundary layer because the shocked solar wind or magnetosheath has a characteristic spectral signature for electrons as well. However, there are magnetopause crossings where low-energy electrons might suggest a depletion layer outside the magnetopause even though the traditional field-rotation signature indicates that this same region is a boundary layer Earthward of the current layer (see Anderson et al., 1993). Our analyses avoided crossings which exhibit such ambiguities.

Pristine magnetopause crossings are magnetopause crossings for which the current layer is well defined and for which there is no adjoining magnetospheric boundary layer as defined above. Although most magnetopause models to date apply to such crossings, few comparisons between such theory and observations of pristine magnetopause crossings have been made because most crossings have an associated magnetospheric boundary layer which significantly affects the applicable boundary conditions for the magnetopause current layer. Furthermore, almost no observational studies of magnetopause microstructure have been done even though key theoretical issues have been discussed for over two decades (Willis, 1971). This is because plasma instruments deployed prior to the ISEE and AMPTE missions did not have the required time resolution and most ISEE investigations to-date have focused on tests of MHD plasma models, especially reconnection.

More recently, many phenomenological and theoretical models have been developed to explain the existence and characteristics of the magnetospheric boundary layers with only limited success to date (see reviews by Lundin, 1988, and Eastman, 1990). The cases with no boundary layer treated in this study provide a contrary set of conditions to those observed with a boundary layer. For the measured parameters of such cases, a successful boundary layer model should predict no plasma penetration across the magnetopause. Thus, this research project provides the first direct observational tests of magnetopause models using pristine magnetopause crossings and provides important new results on magnetopause microstructure and associated kinetic processes.

Research results are documented in the Summary and Conclusions section and, most importantly, in research reports listed in the Grant Publications section below.

SPACECRAFT AND DATA SETS

The AMPTE/CCE spacecraft operated from launch on August 16, 1984 until early 1989. It was in a near equatorial orbit with an apogee of 8.8 R_E and a 15.6 h period (Figure 1). During disturbed interplanetary and geomagnetic conditions ($K_p > 5$), the spacecraft sometimes traversed the frontside magnetopause region although always at low latitude (< 15°). The spin axis of CCE points roughly sunward and its spin period is about 6 s. A full complement of particle and fields instrumentation was flown as documented by Bryant et al. (1985). The AMPTE/CCE observations presented in this paper were obtained primarily by the Hot-Plasma Composition Experiment (HPCE) (Shelley et al., 1985) and the Magnetic Field Experiment (MAG) (Potemra et al., 1985). With this plasma instrument, two-dimensional measurements of electron velocity distributions are made from 50 eV to 25 keV and, for ion distributions, from near spacecraft potential to 17 keV/e. If the electron angular distributions are assumed to be quasi-isotropic, nominal electron densities can be obtained every 155 ms. Such high time resolution data are used in this paper, limited primarily by easily recognized spin modulation as well as by a 50 eV lower-energy cutoff. However, we regard these nominal electron densities to be a proper proxy of total density variations present near the magnetopause and it is that variation which is of most importance for this paper. Simultaneous MAG measurements are provided every 115 ms which, together with the high time resolution electron data, provides a closely matched set of plasma and field data for high time resolution studies. Higher-energy particle measurements supporting this study were obtained with the Charge-Energy-Mass (CHEM) spectrometer (Gloeckler et al., 1985) and the Medium-Energy Particle Analyzer (MEPA) (McEntire et al., 1985).

The ISEE-1 and -2 spacecraft operated from launch on October 22, 1977 until reentry on September, 26, 1987. They flew together with controlled separation distances in a highly eccentric orbit with an apogee of 22.5 R_E and approximately 29° inclination. Plasma and field observations used for this paper were obtained by the Fast Plasma Experiment (FPE) (Bame et al., 1978) and the Fluxgate Magnetometers (Russell et al., 1978). With the plasma instrument, two-dimensional measurements of ion and electron velocity distributions are made at 16 energies at each of 16 azimuths, integrated over +55° of elevation angle relative to the ecliptic, in one satellite rotation of 3 s. The measurement cycle is repeated every spin in high data rate and every fourth spin in low data rate. The Fluxgate Magnetometers provide a field vector every 250 ms when in low data rate and 63 ms in high data rate; crossings plotted in this paper are all high data rate.

AMPTE/CCE and ISEE 2 magnetopause crossings used in our study are listed in the Appendix including crossing times and locations. For the CCE data set, all orbits were examined from launch in August, 1984 through the end of mission in early 1989. However, for ISEE 2, only magnetopause crossings during the first 15 months

of operation were evaluated from launch in October, 1977, through December, 1978. The CCE spacecraft has a low inclination orbit which results in crossing latitudes that are all less than 15°. However, local time coverage by CCE is very limited for such crossings and most occur near local noon because that is where a crossing within its 8.8 R_E apogee is most likely. In contrast, the high-inclination orbit of ISEE 2 resulted in magnetopause crossings ranging from 8° to 23° latitude for our study. Fortunately, ISEE 2 coverage is excellent at all local times although crossings close to local noon are typically more than 15° from the magnetic equator. Overall, the combined CCE and ISEE 2 crossing sets provide excellent coverage of the magnetopause at relatively low latitudes from local noon to beyond the dawn-dusk meridian. The magnetic field data are all analyzed by a standard minimum variance analysis method developed by Sonnerup and Cahill (1967) and Siscoe et al. (1968).

A search for no-boundary layer cases was also made in the AMPTE/IRM data set but only one case was found (see section below on "Listings of No Boundary Layer Cases"). IMP 6 and other earlier satellite data sets had plasma instruments with longer cycle times which eliminate the possibility of examining no boundary layer cases with any confidence. The present study pushes the sampling capabilities of AMPTE/CCE to the limit (using non-spin averaged electron samples). Unfortunately, the HPCE ion instrument had a long cycle time (three minutes) which only allowed rough estimates of ion data on both sides of the magnetopause but provided no resolution of the density gradient itself. Only instruments having cycle times of one second or less can begin to resolve pristine magnetopause crossings; such instruments are just beginning to appear with the ISTP program. Our research on pristine magnetopause crossings reveals only very partially the richness and complexity of magnetopause microstructure and kinetics.

PRISTINE MAGNETOPAUSE CROSSINGS

Our research focused primarily on the microstructure of pristine magnetopause crossings based on high-resolution particle and field data obtained by the AMPTE/CCE and ISEE 2 spacecraft. These crossings have no adjoining magnetospheric boundary layer or, at most, a low-density plateau. Ten such CCE crossings were identified and, due to the AMPTE orbit, they all occur at low latitude (< 15°). Crossings were identified from near the dawn meridian to about 1300 hours local time. Although spin-averaged plasma moments are sampled with 6–second resolution, non-spin averaged electron spectra are sampled every 155 ms, thus enabling high-time-resolution studies of magnetopause microstructure at scales comparable to the high-resolution magnetometer data which have a 115–ms sampling period. In some cases, the electron distributions are approximately isotropic so that these non-spin-averaged moments closely reflect true density variations. Although only one spacecraft is used, approximate values of magnetopause thickness are obtained by using remote sensing information

available in selected energetic ion channels. For the seven crossings analyzed in this way, the magnetopause thickness is found to be approximately 1 to 3 ion gyroradii. For several cases analyzed, the density gradient is found to be very sharp at times with scale lengths down to only a few plasma skin depths. The primary density gradient is also found to usually occur near the inner edge of the current layer, especially for crossings near local noon. Low-frequency magnetic waves are observed from 0.5 to 1 Hz (roughly the ion cyclotron frequency). Close to the magnetopause, some enhancements of broad-band electrostatic noise are observed as well (unfortunately, the measurements are not very reliable as noted in the "Power Spectra and Ratios" section below). These results indicate that low- and high-frequency plasma waves are created in the presence of very steep plasma gradients within the magnetopause current layer and that these waves can act back on the particle distributions to reduce the steep gradients.

A classic example of a pristine magnetopause crossing is presented in Figure 2. This CCE magnetopause crossing near the subsolar point shows a very clean field rotation in the maximum field component, B_i, whereas the normal field component, B_k, remains constant near zero. However, B_k is not sufficiently steady to specify its type as an MHD discontinuity. Further, the intermediate field component, B_j, exhibits a bimodal pattern which indicates the presence of a filamentary current structure within the magnetopause. The magnetopause current layer is identified by the field rotation interval from 82215 sec to 82222.5 sec within which the electron density remains at magnetosheath levels. Plotted electron "densities" are only for electrons above 50 eV and are not spin averaged; nevertheless, spin modulation at the 6–sec spin period is not noticeable. At the inner edge of the magnetopause, the density drops more than three orders of magnitude in less than 0.8 sec to magnetospheric levels based on data samples taken every 155 ms. Farther earthward, there is no evidence for any magnetosheath-like plasma indicating the presence of a boundary layer. The steep density gradient observed has a scale length intermediate between electron scale and one ion gyroradius (Eastman et al., 1994, 1995).

For all pristine magnetopause crossings observed in the subsolar region, we find that the overall magnetopause remains well-defined by the shear in magnetic field but that the primary density drop from magnetosheath to magnetospheric levels occurs on the Earthward side of the current layer over a scale length that is often less than 20% of the current layer width. Several additional examples of magnetopause microstructure are shown in Figures 3 and 4 which contain detailed data for seven additional cases. Some of the density plots show a spin-period variation because they are not spin-averaged densities. In addition, these "densities" are only for electrons above 50 eV and thus provide only a proxy for total density. However, they still show clearly the substructure of the magnetopause that is the focus of our study. In every case, the primary density gradient is located on the Earthward side of the overall magnetopause

and the density gradient scale length is systematically less than the current scale length. Some cases (e.g., 335/84) show a clear low-density plateau which could be interpreted as an incipient boundary layer. However, these are of sufficiently low density so that each case is still appropriately treated as a no-boundary layer case with fairly clean separation of the current layer itself. Observed density gradients range between electron scale (~1 km plasma skin depth) and ion Larmor radii (10 to 50 km for the CCE cases). Table 1 lists basic data for the AMPTE/CCE crossings including time, magnetic local time, radial distance, scale length of the current layer (L) in units of ion gyroradii (R_g), local electron anisotropy, and the time interval of any low-density plateau or "brief quasi-boundary layer." No other local parameter was found to correlate with the sense of electron anisotropy which is probably driven by both local and non-local conditions.

LOCAL TIME DEPENDENCE

The local time distribution of ISEE 2 pristine magnetopause crossings is shown in Figure 5. Only ISEE data are used for this purpose because that spacecraft provides the most uniform local time coverage. Pristine magnetopause crossings are observed at all local times and constitute between 3% to 23% of total crossings observed within different local time sectors. In support of these ISEE results, pristine magnetopause crossings are observed by CCE at all local times at which the spacecraft crossed the magnetopause, from 8 to 13 hours MLT. For the ISEE 2 results, occurrence ratios peak near 9 and 17 hours MLT and have a minimum near 13 hours MLT. Statistics are best on the frontside from 8 to 18 hours MLT and, within this region, the likelihood of pristine magnetopause crossings is lowest near noon or slightly post noon. On average, over the frontside magnetosphere, pristine magnetopause crossings occur for 10% of all crossings. For 75% of magnetopause crossings when the average magnetosheath field is well defined, 60 percent are associated with $-B_z$ in the nearby magnetosheath, whereas only 15% are associated with $+B_z$. Most importantly, pristine magnetopause crossings occur at all local times and are not limited to the subsolar region (Eastman et al., 1994).

We have compared magnetic field and density and have found a systematic difference in magnetopause microstructure with local time. This local time dependence is illustrated in Figure 6 which shows log-scale densities and magnetic field profiles in linear scale for eight sample magnetopause crossings displayed sequentially in magnetic local time. These plots have been scaled to a constant width for the magnetopause to aid in comparing profiles of density and magnetic field. The magnetopause has been identified in each case (and marked with vertical lines) based on all three field components although only the maximum variance component is plotted here. A time interval of 10 seconds is shown below each plot for comparison.

As confirmed by inspection of Figures 3, 4, and 6, density-gradient scale lengths are often comparable to and rarely less than 1/2 of the current-layer scale length for magnetopause crossings more than 1–2 hours local time away from noon. However, most crossings within one hour local time of the subsolar point exhibit a density-gradient scale length less than 20% of the current-layer scale length. For the first three cases, all near local noon, the density gradient scale length is much shorter than the magnetopause interval whereas these scale lengths are comparable for the last three cases far from local noon. The CCE and ISEE cases in between at 10.1 and 9.1 MLT are intermediate in this scale length comparison. Thus, magnetopause has a clear local-time dependence in gradient and current-layer scale lengths which represents an important new test of magnetopause models (Eastman et al., 1995).

Fine structure in the magnetic field profile is often present as well. This is especially dramatic in the CCE magnetopause crossing of day 320 of 1984 where several sharp gradients occur within the overall current layer transition. In this case only, the intermediate variance component is used in Figure 6 because it shows the overall current layer more clearly than the maximum variance component. The day 343/77 crossing of ISEE 2 has high-speed plasma flow (not shown) near the inner portion of the current layer. This location for the high-speed flow is the same as that reported for accelerated plasma flows in Gosling et al. (1986). Such accelerated flows are often confined to the current layer consistent with recent hybrid simulations of a reconnection layer along the flank magnetopause (Lin and Lee, 1994). The other two high-data rate ISEE 2 crossings do not have this high-speed flow signature.

ION COMPOSITION AND PRESSURE BALANCE

Most measurements of the magnetopause region are made only with electron and proton measurements. However, recent ion composition measurements have revealed many important results including the first direct evidence for the overlap of solar wind and ionospheric ions within the boundary layer (Eastman et al., 1990, 1991). Extending the application of such ion composition measurements, we evaluated all plasma and field components of the total pressure across the magnetopause for the six AMPTE/CCE crossings having a full set of plasma and field parameters including electrons, energetic ions and composition. "Hot" electrons are defined as those summed by the electron instrument from 50 eV to 25 keV and "cold" electron densities are obtained by assuming a quasi-neutral plasma and subtracting the hot electron densities from observed ion densities. Nominal cold electron temperatures of 10 eV and 30 eV were assumed for the magnetosheath and magnetosphere, respectively. All particle data below 17 keV are derived from the HPCE instrument; all data above 17 keV are obtained from the CHEM instrument. Summing all pressure components in Table 2 leads to an average change of less than 14% in total pressure across the magnetopause which is within experimental errors (Eastman et al., 1995).

Previous estimates of total pressure near the magnetopause have often failed to yield balance across the magnetopause although, during any arbitrary crossing, one is not likely to observe a brief interval of dynamic imbalance. These earlier estimates were often based on only integrating the magnetic field and low-energy hydrogen components which usually dominate total pressure. However, Table 2 shows that electrons, He^{++} and even field stress can be important in providing detailed balance. In most cases, energetic ions (>17 keV) have very small pressure contributions except for protons on the magnetospheric side in three cases. We found that finite pressure from field stress, $B\Delta B$, was high in two crossings (320/84 and 335/84) for which it was an important part of total pressure balance. This demonstrates that variations along the magnetopause boundary can be very large at times which undermines the application of tangential stress balance and minimum variance calculations which assume no such variation.

Percentage contributions to total pressure are shown Table 3 for both the magnetosheath and magnetospheric side of the magnetopause, based on an average over the six crossings used for Table 2. The combined hot and cold electron components can approach 10% of the total pressure in the magnetosheath. Ion species other than hydrogen can contribute an additional 13% on the magnetospheric side (primarily from high-energy H^+) and 10% on the magnetosheath side (primarily from He^{++}). Thus, electron data and full-energy composition measurements are needed to fully evaluate pressure balance at the magnetopause.

MINIMUM VARIANCE CALCULATIONS

Minimum variance calculations were run in detail on all AMPTE/CCE magnetopause crossings without a boundary layer. The results are summarized in Table 4. The minimum variance technique of Sonnerup assumes a finite normal component for the magnetic field at the magnetopause whereas the Siscoe technique assumes a zero normal component. A variety of nested time intervals were calculated using both techniques to determine solutions with good confidence levels and the highest ratio of the maximum to minimum component, Most calculations are compatible with a tangential discontinuity (zero normal component) with three cases potentially consistent with a rotational discontinuity (finite normal component).

The minimum variance calculations usually had high rms errors in the normal component even when good max/min ratios were achieved. If the crossings occurred near the diffusion region for reconnection (which we suspect in several cases), the minimum variance calculation could show a zero normal component even in the presence of reconnection (which should always be associated with a finite normal component away from the diffusion region). Thus, minimum variance analysis does not provide a clear test of tangential discontinuity vs. rotation discontinuity and reconnection geometry in these cases. Combined with the uncertainty in the

calculations and the observed magnetopause microstructure (imbedded filamentary currents, etc.), it was decided not to include these results in any of the published reports. As noted above in the section on pressure balance, field stress can sometimes be large which indicates significant variation along the boundary. Such variations undercut the basic assumptions of minimum variance calculations. Such calculations also assume that the boundary is effectively stationary during the entire time of measurement. Our measurements of imbedded filamentary structures in the magnetopause at high-time resolution suggest that the magnetopause is rarely stationary and that the minimum variance procedure should only be used as a rough guideline and not a definitive measure of magnetopause type or structure. This qualification is especially important near local noon where we observed very sharp density gradients at scale lengths between electron scale and ion Larmor radii. Under such conditions, the magnetopause is probably never stationary and kinetic instabilities are likely to be important yet highly variable.

Key References on Minimum Variance Techniques:

Lepping and Behannon on Minimum Variance Errors (JGR 85, 4695, 1980)
Siscoe et al. on Siscoe technique (JGR 73, 61, 1968)
Siscoe and Suey, on Significance criteria (JGR 77, 1321, 1972)
Sibeck et al., on Significance tests (JGR, 90, 4013, 1985)
Sonnerup and Cahill, on Sonnerup technique (JGR 73, 1757, 1968)
Sonnerup and Cahill, on Sonnerup technique (JGR 72, 171, 1967)

POWER SPECTRA AND RATIOS

Using the AMPTE/CCE MAG instrument, we examined the magnetic field power spectra at high resolution (analysis routines courtesy of Dr. B. Anderson, JHU/APL). Power spectra for data intervals in the magnetosheath (Sh) and magnetosphere (Sp) adjoining the CCE magnetopause cases are shown in Figure 7. The intermediate (B2) and minimum variance (B3) field components were used. Both B3 and the B2/B3 ratio showed a distinct power spectra peak near the magnetopause at about 0.4 to 1 Hz.

Data from the plasma wave instrument (PWE) on CCE were also evaluated and plotted (see Figure 8). These showed magnetic enhancements in the 1–2 Hz range, effectively consistent with the MAG measurements since this was PWE's lowest channel. Some promising electric field enhancements were found in the PWE 100 Hz channel local to the magnetopause and associated with high density gradients. However, the PWE data were not used for publication because of problems in data quality (high noise and possible contamination).

ENERGETIC PARTICLE MEASUREMENTS

Energetic particle measurements from both the AMPTE/CCE MEPA and CHEM instruments were used for flux estimates. Figure 9 illustrates how clearly the basic boundaries appear when sampling ion composition. Although the instrument cycle time for composition is too slow for detailed magnetopause analysis, the larger context for the boundary crossings is clear. Ionospheric ions dominate within the magnetosphere and solar wind ions dominate outside of it. In the presence of a boundary layer (absent in this case), these ion species always overlap (Eastman et al., 1990). It is common to observe some leakage of ionospheric ions into the nearby magnetosheath (see prior to 0550 UT in the Figure). However, transport inward across both the magnetopause and boundary layer is essentially not observed except for occasional "Mixed Region" conditions (Eastman and Christon, 1995).

The CCE MEPA instrument was used for studies of angular distributions and the sounding of boundaries. Angular distributions of energetic particle flux near the magnetopause were evaluated to check for any systematic dependence on IMF Bz or any other plasma or field parameters. No such systematic dependence was found. All CCE crossings analyzed showed enhanced energetic particle fluxes, presumably of magnetospheric origin, in the magnetosheath near the magnetopause. Thus, presence or absence of a locally-observed boundary layer is not correlated with the presence or absence of energetic particle leakage into the nearby magnetosheath. Some minor leakage at all times could be associated with finite ion gyroradius effects at the boundary.

The energetic particle sounding method was applied to the five AMPTE/CCE magnetopause crossings for which all required data was available. The inferred magnetopause thickness in units of plasma ion gyroradii ranged from 1.4 to 3.4 (Table 1). The CCE crossings analyzed in this paper are all cases of high plasma beta in the nearby magnetosheath. In a recent survey using ISEE data, Le and Russell (1994) found that magnetopause thickness is smaller for such high beta conditions. They report magnetopause thicknesses of 2–4 ion gyroradii, essentially the same result as derived for the CCE cases.

SUMMARY AND CONCLUSIONS

Magnetopause crossings without any substantial boundary layer are found to occur at all local times and such crossings constitute about 10% of all magnetopause crossings sampled by the CCE and ISEE 2 satellite. The overall magnetopause remains well-defined by the shear in magnetic field. When the average magnetosheath field is well defined, 60% of such pristine magnetopause crossings are associated with $-B_z$ in the nearby magnetosheath whereas only 15% of such crossings are associated with $+B_z$.

Analysis of high-resolution density and magnetic field profiles for various magnetopause crossings reveals important fine structure. The density-gradient scale length is often comparable to and rarely less than 1/2 of the current-layer scale length for magnetopause crossings more than 1–2 hours local time away from noon. However, most crossings within one hour local time of the subsolar point exhibit a density-gradient scale length less than 20% of the current-layer scale length.

Energetic ions can be used to scale distances by remotely sensing the magnetopause with their large orbits of gyration. Using this method, the density-gradient scale lengths were often observed to be significantly shorter than one ion gyroradius and sometimes close to the electron skin depth. Magnetopause crossings often exhibit fine structure and gradients on scale lengths much smaller than the scale length of the current layer, especially for crossings near local noon. Earthward of the current layer, in 7 out of the 10 CCE satellite crossings analyzed, a brief low-density plateau is observed and these plateaus all have sharp gradients and small-scale structure. These low-density structures are not substantial boundary layers and represent, at most, the incipient formation of boundary layer plasma earthward of the current layer.

Detailed sums of all plasma and field pressure components were calculated for six of the AMPTE/CCE crossings and the total pressure change observed across the magnetopause is less than 14% on average, which is within experimental errors. Pressure balance calculations to date have usually been based on only integrating the magnetic field and low-energy hydrogen components. Our results indicate that such calculations can be low by 10% or more due to contributions by electrons or ions other than low-energy protons. Thus, electron data and full-energy composition measurements may be necessary for some crossings when evaluating pressure balance at the magnetopause.

Various processes for solar wind penetration of the magnetopause have been proposed to explain the boundary layer usually observed Earthward of the magnetopause (Lundin, 1988) and such penetration has been unambiguously demonstrated using ion composition measurements (Eastman et al., 1990). Reconnection is normally the candidate of choice. Lin and Lee (1994) used hybrid simulations to determine properties of the reconnection layer in the presence of shear flow. For all of the AMPTE/CCE cases, magnetosheath flow speeds are small compared to the difference in Alfvén

speed across the magnetopause. Under this condition, the rotational discontinuity is on magnetosheath side of the reconnection layer. Thus, our magnetopause crossings without a boundary layer clearly have no reconnection layer local to the satellite crossing location. Impulsive plasma penetration through a tangential discontinuity can result in boundary layer plasma under certain conditions as shown by Savoini et al. (1994) based on two-dimensional hybrid simulations. Plasma interactions with lower hybrid waves near the magnetopause can lead to localized field structures and enhanced diffusion rates through turbulence (Shapiro et al., 1994). In each case, the no-boundary layer cases treated in this paper represent conditions under which these processes should not produce a boundary layer.

Neither a reconnection layer or any other type of boundary layer is observed in our magnetopause crossings except for the very thin and highly structured plateau signatures which we do not consider as normal boundary layers and, at most, are signs of the incipient formation of a boundary layer. Whatever produces the boundary layer must be at least locally absent. One possibility is that reconnection is locally present but that the reconnection layer is not which can only happen if the satellite is crossing directly through the diffusion region. Given that only 10% of all crossings are without a boundary layer (Eastman et al., 1994), it may be possible that a significant fraction of such cases are direct crossings of diffusion regions.

Early modeling done for this research project used 1–D hybrid simulations (Cargill and Eastman, 1991). Comparing observations with these simulation results demonstrated that the magnetopause cannot be adequately modeled with any simulation approach less than two dimensional. In contrast, simulations by Prof. James Drake and colleagues of the University of Maryland, inspired by this research grant on no-boundary layer observations, have made significant progress with state-of-the-art 3–D simulations. Both the fine structure that we observe and the possibility of direct crossing of diffusion regions are suggested by their 3–D simulations of the current layer and associated turbulence by Drake et al. (1994a). More recently, these simulations have incorporated full electromagnetic effects (Drake et al., 1994b, 1995). They find current convective instability to be the dominant process for current transport near the magnetopause. Whistler waves are driven unstable by the current gradient at the magnetopause which maintains an overall width comparable to or larger than an ion gyroradius. The collisionless plasma current layers are not simple laminar structures in the 3–D simulations. Instead, they breaakup into filaments of electron streams with a characteristic transverse width roughly equal to the electron plasma skin depth. Drake et al. (1994a,b) suggests that these narrow current layers become turbulent and filamentary. Imbedded filamentary current structures within the magnetopause are common in our AMPTE/CCE no-boundary layer crossings based on the common bimodal signature observed in the intermediate magnetic field values derived from a minimum variance analysis. In some cases, such filamentary currents may offset the prevailing

turbulence by linking up to produce flux transfer events (FTEs) that directly connect the geomagnetic and interplanetary fields, leading to macroscopic changes near the boundary and contributing to formation of the magnetospheric boundary layer (Lee, 1991). The enhanced presence of magnetopause microstructure with $-B_z$ is also consistent with this model for collisionless reconnection at the magnetopause.

Extremely sharp density gradient and filamentary current structures are observed at scale lengths less than ion gyradii and down to electron scale lengths as predicted in the Drake et al. model. This feature becomes most clearly resolved by analyzing magnetopause crossings without a boundary layer because then the short density-gradient scale length can be easily compared to the overall magnetopause current layer width. The associated spectrum of electromagnetic waves predicted by the current convective instability is broadband and extends from the ion cyclotron frequency up to the electron cyclotron frequency. Such a spectrum is commonly observed at the magnetopause as reviewed in detail by Thorne and Tsurutani (1991). Thus, this model for the current convective instability compares favorably with our high-resolution observations of magnetopause microstructure near the subsolar region. As plasma convects around towards the flanks, the source of free energy goes away as gradients in current and density are reduced, instabilities are turned off, and the plasma relaxes to a state of comparable scale lengths for density and current gradients in no-boundary layer crossings, as observed.

BIBLIOGRAPHY

Anderson, B. J., and S. A. Fuselier, Magnetic pulsations from 0.1 to 4.0 Hz and associated plasma properties in the Earth's subsolar magnetosheath and plasma depletion layer, J. Geophys. Res., **98**, 1461, 1993.

Bame, S. J., J. R. Asbridge, H. E. Felthauser, J. P. Glore, G. Paschmann, P. Hemmerich, K. Lehmann, and H. Rosenbauer, ISEE 1 and ISEE 2 fast plasma experiment and the ISEE-1 solar wind experiment, IEEE Trans. on Geosci. Electron. **GE-16**, 216, 1978.

Bryant, D. A., S. M. Krimigis, and G. Haerendel, Outline of the active magnetospheric particle tracer explorers (AMPTE) mission, IEEE Trans. on Geosci. and Remote Sensing **GE-23**, 177, 1985

Cargill, P. and T. Eastman, The structure of tangential discontinuities, 1. Results of hybrid simulations, J. Geophys. Res., 96, 13773–13779, 1991.

Drake, J. F., Jr., J. Gerber, and R. G. Kleva, Turbulence and transport in the magnetopause current layer, J. Geophys. Res., **99**, 11,211, 1994a.

Drake, J. F., Jr., R. G. Kleva, and M. E. Mandt, The structure of thin current layers: implications for magnetic reconnection, *Phys. Rev. Lett*, **73**, 1251, 1994b.

Drake, J. F., Jr., Magnetic reconnection: a kinetic treatment, in The Physics of the Magnetopause, P. Song, B. Sonnerup, and M. Thomsen, eds., AGU, Washington, D.C., in press, 1995.

Eastman, T. E., E. W. Hones, Jr., S. J. Bame, and J. R. Asbridge, The magnetospheric boundary layer: Site of plasma, momentum and energy transfer from the magnetosheath into the magnetosphere, *Geophys. Res. Lett.*, **3**, 685, 1976.

Eastman, T. E., Transition regions in solar system and astrophysical plasmas, IEEE Trans. Plasma Science, Vol. 18, No. 1, 18–25, 1990.

Eastman, T. E., E. A. Greene, S. P. Christon, G. Gloeckler, D. C. Hamilton, F. M. Ipavich, G. Kremser, and B. Wilken, Ion composition in and near the frontside boundary layer, *Geophys. Res. Lett.*, **17**, 2031, 1990.

Eastman, T. E., Recent ion composition results in the magnetopause region, in Physics of Space Plasmas (1991), SPI Conference Proceedings and Reprint Series, Number 10, T. Chang, G. B. Crew, and J. R. Jasperse, eds., Scientific Publishers, Cambridge, MA, pp. 209–218, 1991.

Eastman, T. E., B. Anderson, P. Cargill, S. Fuselier, and J. Gosling, Microstructure of the magnetopause, in The Initial Results from STEP Facilities and Theory Campaigns, Proceedings of the 1992 STEP Symposium/5th COSPAR Colloquium, D. Baker, V. Papitashvili, and M. Teague, editors, Pergamon Press, Oxford, UK, 1994.

Eastman, T. and S. P. Christon, Ion composition and transport near the Earth's magnetopause, in The Physics of the Magnetopause, P. Song, B. Sonnerup, and M. Thomsen, eds., AGU, Washington, D.C., in press, 1995.

Eastman, T. E., D. C. Hamilton, S. A. Fuselier, and J. T. Gosling, Magnetopause crossings without a boundary layer, submitted to *J. Geophys. Res.*, Jan. 1995.

Fritz, T. A., and S. C. Fahnenstiel, High temporal resolution energetic particle soundings at the magnetopause on November 8, 1977 using ISEE-2, *J. Geophys. Res.*, **87**, 2125, 1982.

Gloeckler, G., F. M. Ipavich, W. Studemann, B. Wilken, D. C. Hamilton, G. Kremser, D. Hovestadt, F. Gliem, R. A. Lundgren, W. Rieck, E. O. Tums, J. C. Cain, L. S. Masung, W. Weiss, and P. Winterhof, The charge-energy-mass spectrometer for 0.3–300 keV/e ions on the AMPTE CCE, IEEE Trans. on Geosci. and Remote Sensing **GE-23**, 234, 1985.

Gosling, J. T., M. F. Thomsen, S. J. Bame, and C. T. Russell, Accelerated plasma flows at the near-tail magnetopause, J. Geophys. Res., 91, 3029, 1986.

Hall, D. S., C. P. Chaloner, D. A. Bryant, D. R. Lepine, and V. P. Tritakis, Electrons in the boundary layers near the dayside magnetopause, J. Geophys. Res., 96, 7869, 1991.

Hones, E. W., Jr., J. R. Asbridge, S. J. Bame, M. D. Montgomery, S. Singer, and S.-I. Akasofu, Measurements of magnetotail plasma flow made with VELA 4B, *J. Geophys. Res.*, **77**, 5503, 1972.

Le, G., and C. T. Russell, The thickness and structure of high beta magnetopause current layer, *Geophys. Res. Lett.*, **21**, 2451, 1994.

Lee, L. C., The magnetopause: A tutorial review, in *Physics of Space Plasmas (1990)*, SPI Conference Proceedings, Number 10, T. Chang, G. B. Crew, and J. R. Jasperse, editors, Scientific Publishers, Inc., 1991.

Lin, Y., and L. C. Lee, Reconnection layer at the flank magnetopause in the presence of shear flow, *Geophys. Res. Lett.*, **21**, 855, 1994.

Lundin, R., On the magnetospheric boundary layer and solar wind energy transfer into the magnetosphere, *Sp. Sci. Rev..*, **48**, 263, 1988.

McEntire, R. W., E. P. Keath, D. E. Fort, A. T. Y. Lui, and S. M. Krimigis, The medium-energy particle analyzer (MEPA) on the AMPTE CCE spacecraft, IEEE Trans. on Geosci. and Remote Sensing **GE-23**, 230, 1985.

Paschmann, G., G. Haerendel, N. Sckopke, H. Rosenbauer, and P. D. Hedgecock, Plasma and magnetic field characteristics of the distant polar cusp near local noon: The entry layer, *J. Geophys. Res.*, **81**, 2883, 1976.

Potemra, T. A., L. J. Zanetti, and M. H. Acuna, The AMPTE CCE magnetic field experiment, IEEE Trans. on Geosci. and Remote Sensing **GE-23**, 246, 1985.

Rosenbauer, H., H. Grunwaldt, M. D. Montgomery, G. Paschmann, and N. Sckopke, HEOS 2 plasma observations in the distant polar magnetosphere: The plasma mantle, *J. Geophys. Res.*, **80**, 2723, 1975.

Russell, C. T., ISEE 1 and 2 fluxgate magnetometers, IEEE Trans. on Geosci. Electron. **GE-16**, 239, 1978.

Shelley, E. G., A. Ghielmettic, E. Hertzberg, S. J. Battel, K. Altwegg von Burg, and H. Balsiger, The AMPTE/CCE hot-plasma composition experiment (HPCE), IEEE Trans. on Geosci. and Remote Sensing **GE-23**, 241, 1985

Siscoe, G. L., L. Davis, Jr., P. J. Coleman, Jr., E. J. Smith, and D. E. Jones, Power spectra and discontinuities of the interplanetary magnetic field: Mariner 4, *J. Geophys. Res.*, **73**, 61, 1968.

Sonnerup, B. U. O., and L. J. Cahill, Magnetopause structure and attitude from Explorer 12 observations, *J. Geophys. Res.*, **72**, 171, 1967.

Thorne, R., and B. Tsurutani, Wave-particle interactions in the magnetopause boundary layer, in *Physics of Space Plasmas (1990)*, SPI Conference Proceedings, Number 10, T. Chang, G. B. Crew, and J. R. Jasperse, editors, Scientific Publishers, Inc., 1991.

Willis, D. M., Structure of the magnetopause, *Rev. Geophys. Sp. Phys..*, **9**, 953, 1971.

GRANT PUBLICATIONS

Eastman, T. E., Recent ion composition results in the magnetopause region, in Physics of Space Plasmas (1991), SPI Conference Proceedings and Reprint Series, Number 10, T. Chang, G. B. Crew, and J. R. Jasperse, eds., Scientific Publishers, Cambridge, MA, pp. 209–218, 1991.

Cargill, P. and T. Eastman, The structure of tangential discontinuities, 1. Results of hybrid simulations, J. Geophys. Res., 96, 13773–13779, 1991.

Eastman, T., B. Anderson, P. Cargill, S. Fuselier, and J. Gosling, Microstructure of the magnetopause, in Initial Results from STEP Facilities and Theory Campaigns, Proceedings of the 1992 COSPAR Colloquium, Pergamon Press, 5, 1994.

Eastman, T. and S. P. Christon, Ion composition and transport near the Earth's magnetopause, in The Physics of the Magnetopause, P. Song, editor, AGU, Washington, D.C., in press, 1995.

Eastman, T. E., D. C. Hamilton, S. A. Fuselier, and J. T. Gosling, Magnetopause crossings without a boundary layer, submitted to *J. Geophys. Res.*, Jan. 1995.

Works Directly Motivated by this Study:

Drake, J. F., Jr., J. Gerber, and R. G. Kleva, Turbulence and transport in the magnetopause current layer, J. Geophys. Res., 99, 11211, 1994a.

Drake, J. F., Jr., R. G. Kleva, and M. E. Mandt, The structure of thin current layers: implications for magnetic reconnection, *Phys. Rev. Lett*, **73**, 1251, 1994b.

Drake, J. F., Jr., Magnetic reconnection: a kinetic treatment, in The Physics of the Magnetopause, P. Song, B. Sonnerup, and M. Thomsen, eds., AGU, Washington, D.C., in press, 1995.

Romero, H. and G. Ganguli, Relaxation of the stressed plasma sheet boundary layer, Geophys. Res. Lett., 21, 645, 1994.

Ganguli, G., H. Romero, and J. Fedder, Interaction between global MHD and kinetic processes in the magnetotail, in Solar System Plasmas in Space and Time, AGU Monograph #84, p. 135, 1994.

Ganguli, G., H. Romero, and P. Dusenbery, The dynamical plasma sheet boundary layer, in Micro- and Mesoscale Phenomena, J. Burch, editor, AGU, Washington, D.C. in press, 1995.

Other Related Publications by the P.I.:

Eastman, T. E., Transition regions in solar system and astrophysical plasmas, IEEE Trans. Plasma Science, Vol. 18, No. 1, 18–25, 1990.

Eastman, T. E., E. A. Greene, S. Christon, G. Gloeckler, D. C. Hamilton, F. M. Ipavich. G. Kremser, and B. Wilken, Ion composition in and near the frontside boundary layer, Geophys. Res. Lett., 17, 2031–2034, 1990.

Eastman, T., Micro- to macroscale perspectives on space plasmas, Physics of Fluids B (Plasma Phgysics), 5, 2671, 1993.

Eastman, T. Magnetosphere, submitted with invitation to The Encyclopedia of Climate and Weather, Oxford University Press, 1994.

Invited Lectures Related to this Study:

Emerging perspectives on the magnetopause and frontside boundary layer, MIT, July, 1990.

Reviews of magnetospheric boundary layers and new results from AMPTE/CCE, SwRI, Dec., 1990.

Ion composition near the daysider magnetospheric boundary, Dartmouth, May, 1991.

Geospace: our laboratory for space plasma kinetics, MIT, Aug., 1992.

Micro- to macroscale processes in Geospace, APS meeting, Seattle, Nov., 1992.

Global coherence and cross-scale coupling in the Earth's magnetosphere, Fall AGU, Dec., 1993.

Composition and microstructure in the magnetopause region, Chapman Conf., San Diego, Mar., 1994.

During the four-year period during which this grant was active, the P.I. presented a total of 24 invited lectures and published 13 papers, including eight as first author. From August, 1991 through January, 1994, Dr. Eastman was on leave-of-absence to the National Science Foundation as Program Director for Magnetospheric Physics [2–1/2 years at NSF and just over 1–1/2 years full-time at the University of Maryland during the active grant period]. While at NSF, Dr. Eastman played the lead role in conceiving and initial forwarding of the important Space Weather Initiative (building on the NSF-STEP initiative that he formulated), managed and expanded the Geospace Environment Modeling (GEM) program, and provided coordination at NSF for all aspects of plasma science and technology.

LISTINGS OF NO BOUNDARY LAYER CASES

The AMPTE/CCE data were analyzed in the ten available no-boundary layer cases to the limits of the available data. ISEE 2 data were used primarily for survey purposes and to evaluate local time dependence of magnetopause microstructure. Only five ISEE 2 magnetopause crossings were found in high-data rate that also had no boundary layer.

Dec. 9 (day 343) 1977, 0502:09 to 0503:17 UT

Dec. 13 (day 347) 1977, 2133:38 to 2134:38 UT

May 31 (day 151) 1978, 1145 to 1150 UT (Gosling et al., 1986; Fig. 3, 4, and 16)

June 10 (day 161) 1978, 1357:30 to 1400:30 UT (Gosling et al., 1986; Fig. 6, 7, and 12)

June 30 (day 181) 1978, 0036:39 to 0037:30 UT

All crossing days showing a no-boundary layer crossing with AMPTE/CCE were also checked with the complementary AMPTE/UKS spacecraft. In only one case, a no-boundary layer crossing was identified by the UKS satellite.

Aug. 28 (day 241) 1984, 1304 UT (published in Hall et al., 1991)

AMPTE/CCE Magnetopause Crossings

DATE	DOY	UT	r(R)	°LAT	MLT	L/Rg
10-6-84	280	0148	7.7	-10.2	11.2	
10-19-84	293	0636	8.8	-11.5	11.9	1.6
11-13-84	318	1613	8.8	7.6	10.0	2.2
11-14-84	319	2355	8.8	-11.1	10.1	
11-15-84	320	1900	7.8	3.7	11.2	
11-30-84	335	0524	6.3	-15.4	11.5	3.4
12-26-84	361	0303	8.8	-13.6	8.1	1.5
2-8-86	039	2250	5.2	6.5	12.9	
2-14-86	045	1530	8.6	13.3	10.8	
4-14-87	104	1334	8.8	3.4	12.6	1.4

Note: L/Rg is the magnetopause thickness in units of ion gyradii.

ISEE 2 Magnetopause Crossings

DATE	DOY	UT	r (R)	°LAT	MLT
11-15-77	319	0614, 0627	12	23	10.4
12-9-77	343	0503	11	22	9.1
12-11-77	345	1435	11	22	8.9
12-13-77	347	2134, 2151	13	22	8.5
12-25-77	359	2232	11	21	8.0
12-30-77	364	1322	14	22	7.2
1-4-78	004	1312	9	18	7.9
2-15-78	046	0834	21	22	≤ 3
5-31-78	151	0630	20	21	19.3
6-10-78	161	1358	21	18	19.7
6-30-78	181	0037	18	15	19.0
6-30-78	181	1927	10	23	15.9
8-8-78	220	0243	13	23	14.0
8-14-78	226	1542	14	10	16.7
8-19-78	231	1038	14	10	16.7
8-24-78	236	0633,0635 0639,0641	12	8	16.3
8-21-78	233	2109	12	8	16.4
8-31-78	243	1017	13	8	15.7
9-3-78	246	0708	11	23	12.0
11-15-78	319	2108	12	4	10.8
12-17-78	351	1302	13	22	5.3

APPENDIX – Grant Data and No-Cost Extension

```
From <@astro.umd.edu,@UMDMVS.umd.edu:PROBMGMT@UMDACC.UMD.EDU> Tue Aug 30 14:32:38 1994
FROM: ORAA%UMDMVS.umd.edu:PROBMGMT@UMDACC.UMD.EDU
TO: EASTMAN@astro.umd.edu, YORKE@IPST.UMD.EDU, galifaro@IPST.UMD.EDU,
        JROBERTS@deans.umd.edu
Subject: Sponsored Project ATS/Account Transaction Summary
Content-Length: 1135
X-Lines: 28

Proj Director: Eastman, Timothy E.
Account Num  : 01-5-26987  Related: NONE        Previous: NONE
S.A.I. Number: 890515-7530
Duration     : 09/01/89 - 12/31/94   Action Taken: No Cost Extension
Proj. Sponsor: (4120) NASA - Headquarters  SPACE PHYSIC
Sponsor's Num: NAGW1848
Project Title: Observations of the Magnetopause Layer:  Cases with.....
Dept. or Unit: (11L080) INST - PHYSICAL SCIENCE & TECH - COLLEGE CMPS

Funds: This Action:           0  * Direct Cost This Action: 0
          Previous:     150,000
      Total Amount:     150,000  Indirect Cost Rate: 46.0% MTDC

Cost Sharing : N/A.

Proj. Reports: Brief, informal Semi-Annual Status Reports and a
               Final Technical Report.
 (Financial reports will be prepared by Contract and Grant Acctng.)

Remarks:
A copy of Supplemenmt No. 7 is attached for Ms. E. Galifaro.
Note:  Per NASA HQ:  This is the lase no-cost extension
permitted under this grant.

Assistance: ORAA          Booker McManus                Phone: 405-6277
            Accounting    Dennis Trimble                Phone: 405-2613

This mail is for notification purposes only. PLEASE DO NOT REPLY.
```

UNIVERSITY OF MARYLAND AT COLLEGE PARK

INSTITUTE FOR PHYSICAL SCIENCE AND TECHNOLOGY

June 21, 1994

Dr. Elden Whipple
Space Physics Division, Code SS
NASA Headquarters
Washington, D. C. 20546

Subject: Request of no-cost extension for grant NAGW-1848

Dear Dr. Whipple:

A 2-1/2 year leave-of-absence to the National Science Foundation, completed in January, has delayed completion on Grant NAGW-1848. We request a six-month no-cost extension to complete work.

Recent progress includes publication of "Microstructure of the Magnetopause" in the COSPAR-STEP Symposium proceedings (Advances in Space Research, Feb., 1994) and submittal of a related paper on "Ion Composition and Transport near the Earth's Magnetopause" (submitted to Physics of the Magnetopause, P. Song, ed., AGU, Washington, D. C., 1994).

Work is continuing on papers concerning "Local time dependence of magnetopause microstructure" and "Pristine magnetopause crossings."

At no additional cost to NASA, continuation of this grant will enable me to further complete the initially-funded scope of work. Thus, we request a six-month no-cost extension for Grant NAGW-1848.

With very best regards,

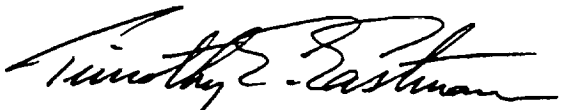

Timothy E. Eastman
Principal Investigator
301-405-4829
301-314-9363 (FAX)
email: eastman@astro.umd.edu

TEE/dm

Table 1. AMPTE/CCE PRISTINE MAGNETOPAUSE CROSSINGS

Date (doy/yr)	Time (UT)	MLT (hrs)	r (R_E)	L(Rg)	Rg(km)	electron anisotropy	brief BL (sec)
280/84	0148	11.2	7.7		24	bi-dir.	19
293/84	0635	11.9	8.8	1.6	54	iso.	14
318/84	1613	10.0	8.8	2.2	27	unidir.	5
319/84	2355	10.1	8.8		30	iso.	8?
320/84	1900	11.2	7.8		21	bi-dir.	
335/84	0524	11.5	6.3	3.4	9	bi-dir.	6
361/84	0303	8.1	8.8	1.5	22	bi-dir.	
039/86	2250	12.9	5.2			iso.	
045/86	1530	10.8	8.6			bi-dir.	19
104/87	1334	12.6	8.8	1.4	40	iso.	3

Table 2. Magnetopause Pressure Balance Calculations

Doy/Yr	280/84	293/84	318/84	319/84	320/84	335/84
$B^2/2\mu_o$	0.4/ 7.2	0.4 / 4.6	1.0 / 3.2	0.6 / 5.4	4.0 / 5.7	15.9 / 37.0
$B\Delta B/2\mu_o$			0 / 0.5	0 / 1.4	0 / 5.7	0 / 5.2
nkT (H^+)	13.5 / 6.7	6.1 / 0.9	4.0 / 0.1	6.4 / .05	8.9 / 0.5	30.6 / 0.9
nkT (hot e^-)	1.6 / 0.3	0.9 / .02	0.4 / .05	0.4 / 0.1	0.2 / .01	0.6 / .01
nkT (cold e^-)	0.2 / .03	.04 / 0	0.1 / 0	0.2 / 0	0.2 / .01	0.6 / .01
nkT (He^{++})	1.3 / 0.2	1.1 / .01	0.6 / .01	1.0 / 0	1.2 / .04	1.2 / .01
nkT (He^+)	0 / .05	0 / .01	.02 / .02	0 / .01	.01 / .04	.02 / .01
nkT (O^+)	.03 / 0.1	0 / .09	.01 / .03	.01 / .05	0 / 0.1	.01 / .09
H^+ (>17keV)	0 / .06	0.4 / 1.3	.01 / 0.1	.01 / 0.2	.04 / 1.5	0.6 / 3.9
O^+ (>17keV)	.01 / 0	.05 / 0.2	0 / 0	0 / .01	0 / 0.2	.01 / 0
He^{++} (>17keV)	0 / 0	0.1 / 0.1	0 / 0	.02 / .01	.02 / 0	.08 / 0.5
He^+ (>17keV)	0 / 0	0 / .01	0 / .01	0 / 0	0 / .06	0 / .03
Total Pressure	17.0 / 14.7	9.0 / 7.1	6.2 / 4.2	8.6 / 7.3	14.5 / 13.9	49.7 / 47.6

All pressure values are in units of 10-9 Pascals. Each ordered pair (x/y) denotes pressures for the magnetosheath and magnetosphere, respectively.

Table 3. Percentage Contributions to Average Pressure

B	H	hot e	cold e	He++	He+	O+	H+ (>17 keV)	O+ (>17 keV)	He++ (>17 keV)	He+ (>17 keV)
MAGNETOSHEATH										
19	61	7.4	1.9	8	0.07	0.06	1.3	0.16	0.42	0.05
MAGNETOSPHERE										
78	9	1	0.06	0.7	0.19	0.66	9	0.91	0.51	0.002

Table 4. AMPTE/CCE Minimum Variance Calculations

DATE	DOY	Magnetopause	λ_I/λ_m	B_n	σ_{Bn}	Type*
10-6-84	280	0148:15-45	21	1.3	3	TD
10-19-84	293	0634:55-0636:10	17	2.0	13	TD
11-13-84	318	1613:21-40	7	-2.1	8	TD
11-14-84	319	2355:28-42	12	1.9	2.4	TD
11-15-84	320	1900:11-17	4.7	92	51	RD?
11-30-84	335	0524:32-44	28	-0.1	14	TD
12-26-84	361	0302:52-0303:06	22	40	48	RD?
2-8-86	039	2250:10-30	10	4.7	47	TD?
2-14-86	045	1530:00-50	27	28	21	RD
4-14-87	104	1334:22-35	14	-10	4	RD

*TD or RD type denotes probable tangential vs. rotational discontinuity

λ_I/λ_m, ratio of maximum to intermediate eigenvalues derived from the minimum variance calculation.

B_n, σ_{Bn} - normal component for B and the one-σ rms error

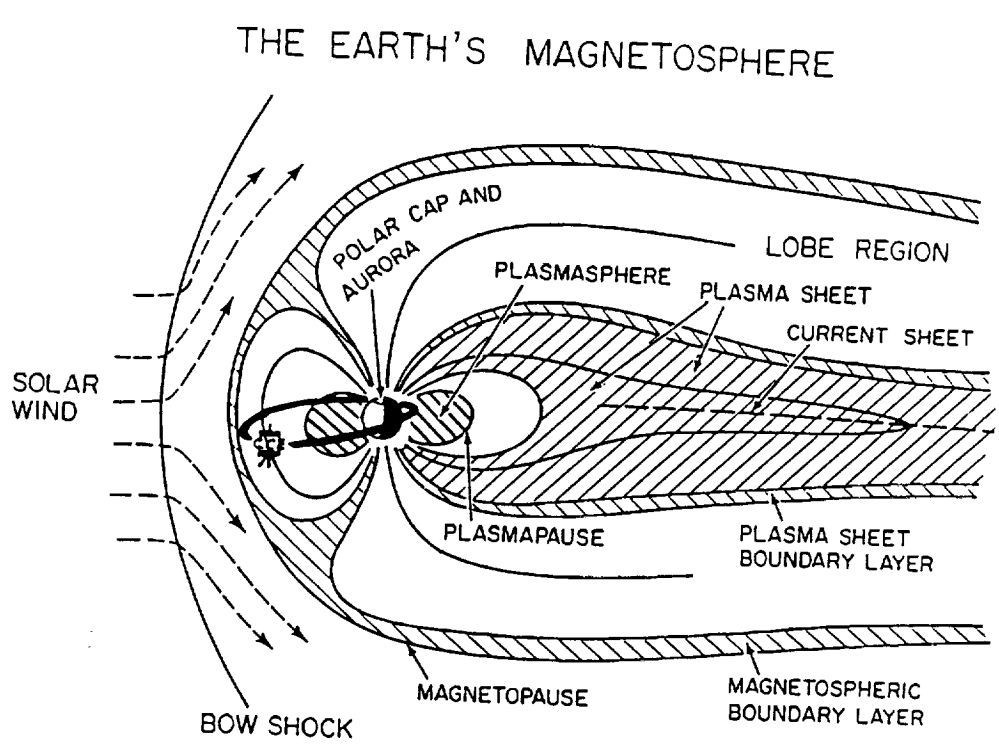

Figure 1. The AMPTE/CCE orbit is illustrated here with a noon-midnight meridian cross section of the mag netosphere. Major plasma domains and boundaries are identified. As the magnetopause moves with changing solar wind conditions, CCE can sample the magnetopause near its 8.8 R_E apogee.

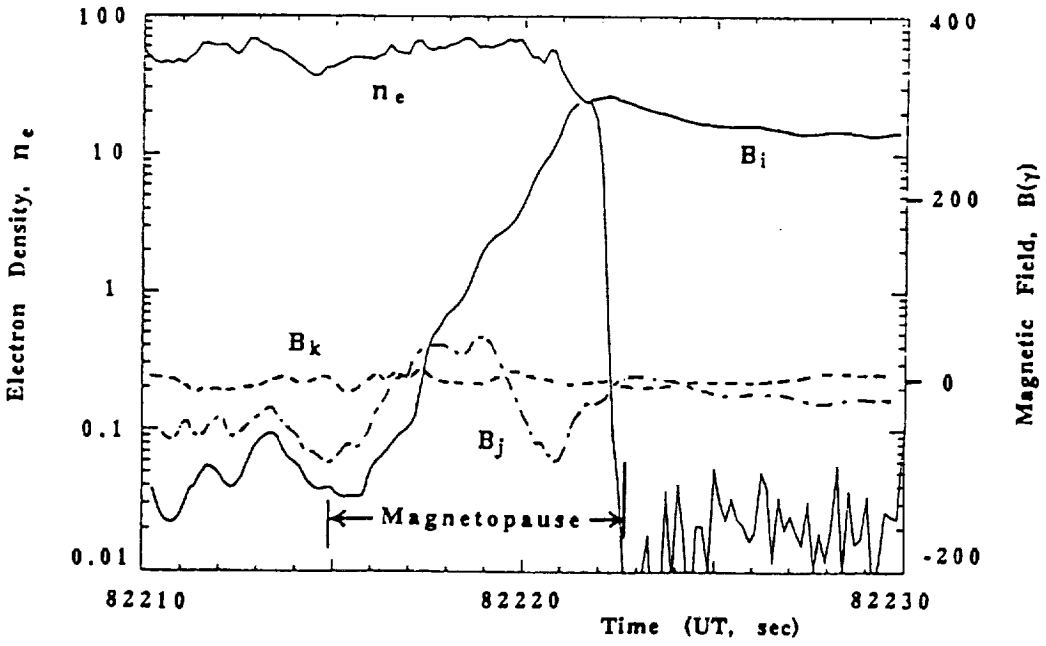

Figure 2. Electron density and magnetic field vs. time for the AMPTE/CCE magnetopause crossing of 8 February 1986 (day 039); mean of minimum component B_k is 4.7γ with 45γ standard deviation.

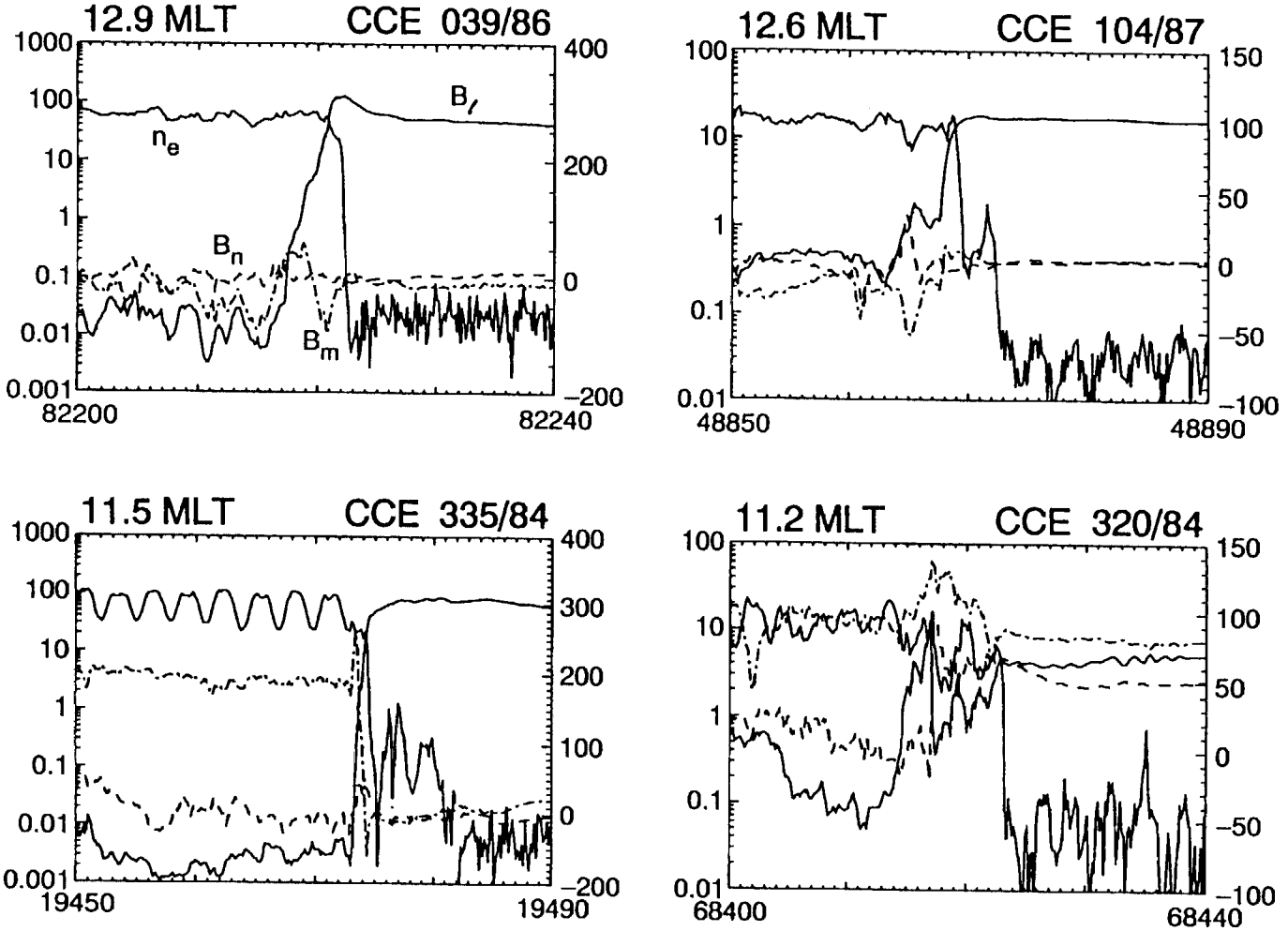

Figure 3. Pristine magnetopause crossings near local noon by the AMPTE/CCE spacecraft. Electron "density" values are integrated above 50 eV and are not spin averaged; spin modulation reflecting the 6–sec spin period is present in the bottom two panels. B_l, B_m, and B_n are the maximum, intermediate, and minimum variance components, respectively, of magnetic field derived from a minimum variance analysis across the magnetopause. [Density scale in cm^{-3} and the left side; magnetic field scale in γ ($=10^{-5}$ gauss) on the right side; time in seconds on the horizontal axes, each tic mark represents one second.]

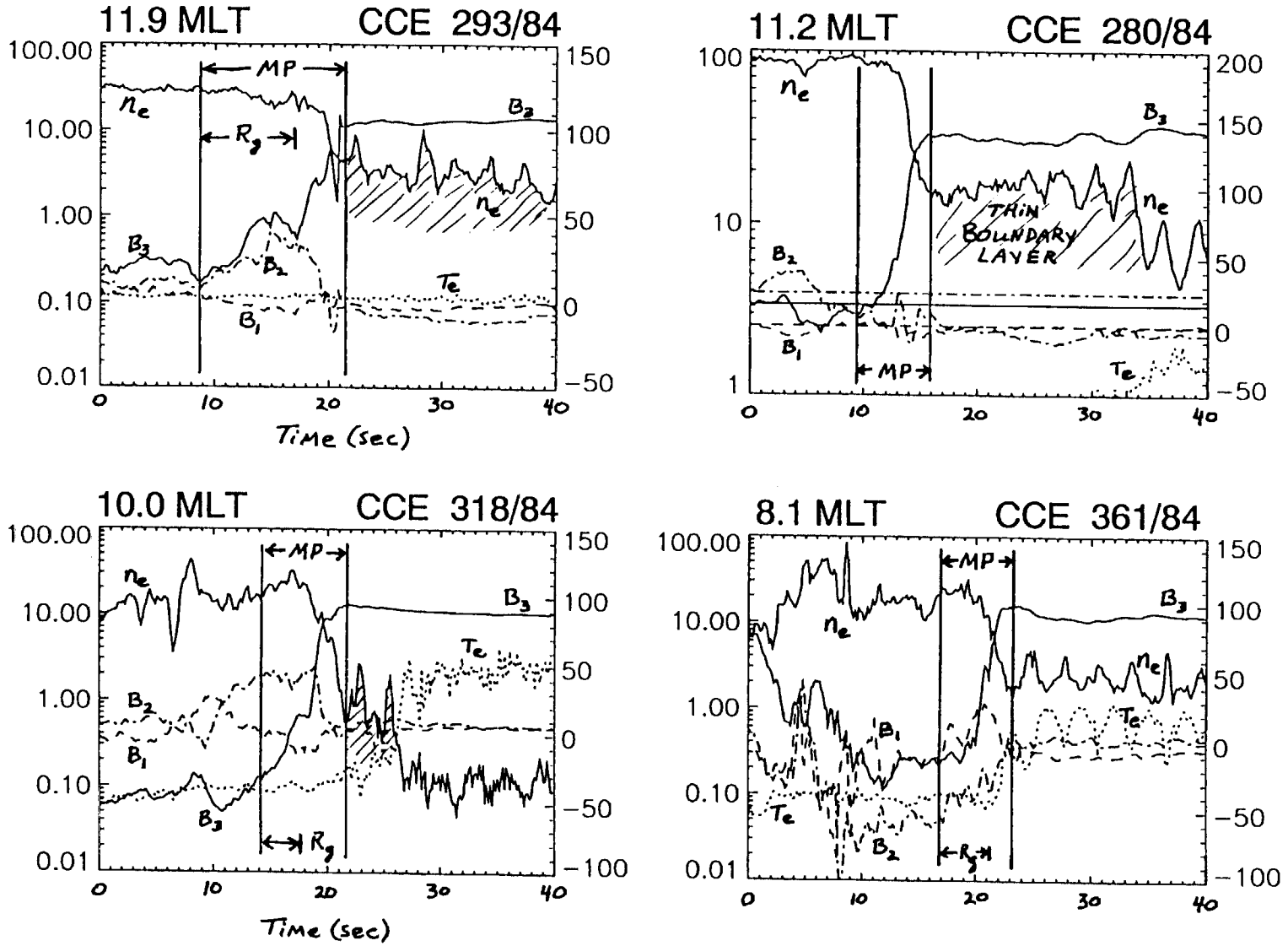

Figure 4. Additional AMPTE/CCE magnetopause crossings are presented here which have either no boundary layer or a very low-density plateau. $B_{1,2,3}$ here denote the $B_{n,m,l}$ components of Figure 3.

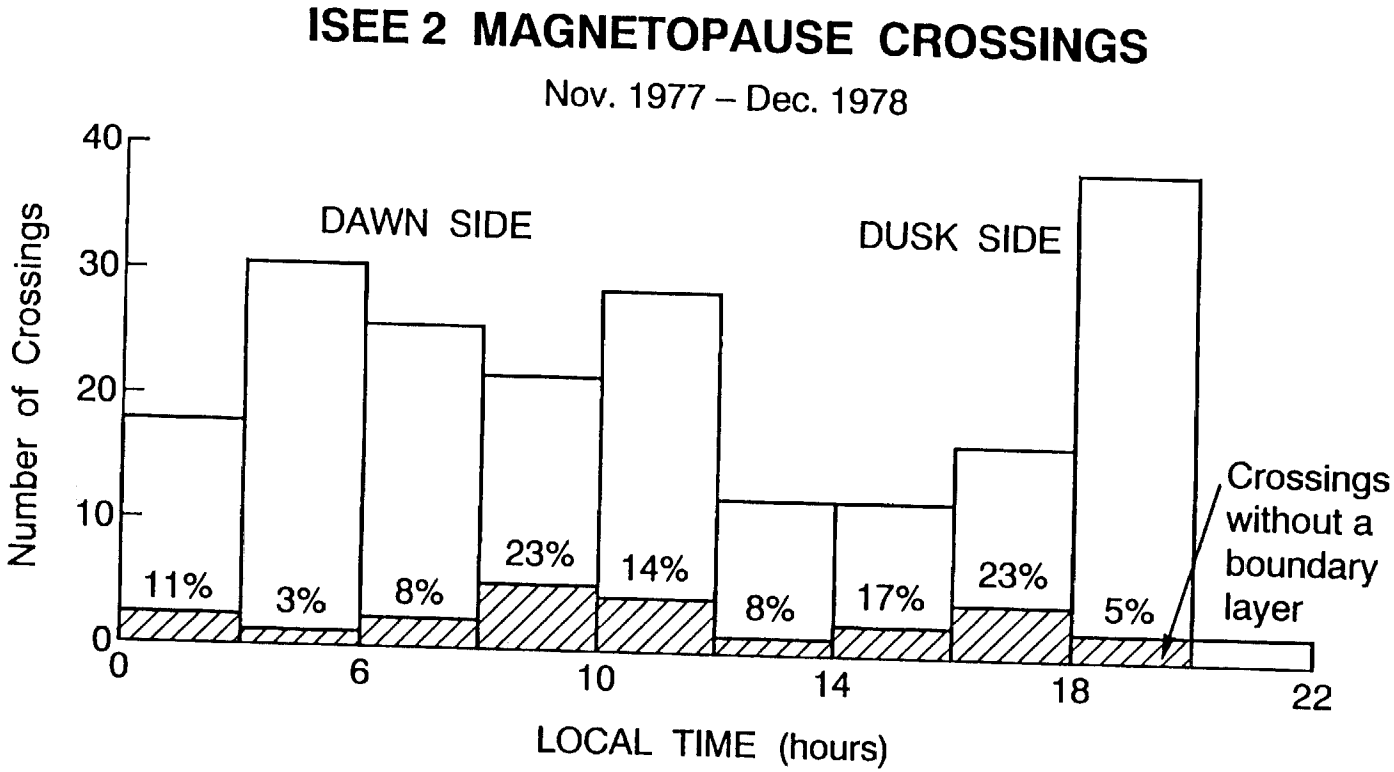

Figure 5. Local time distribution of ISEE 2 satellite crossings is presented as sampled during its first 15 months of operation. Magnetopause crossings without a boundary layer are shown (cross-hatched) with percentages of pristine crossings and total crossing numbers.

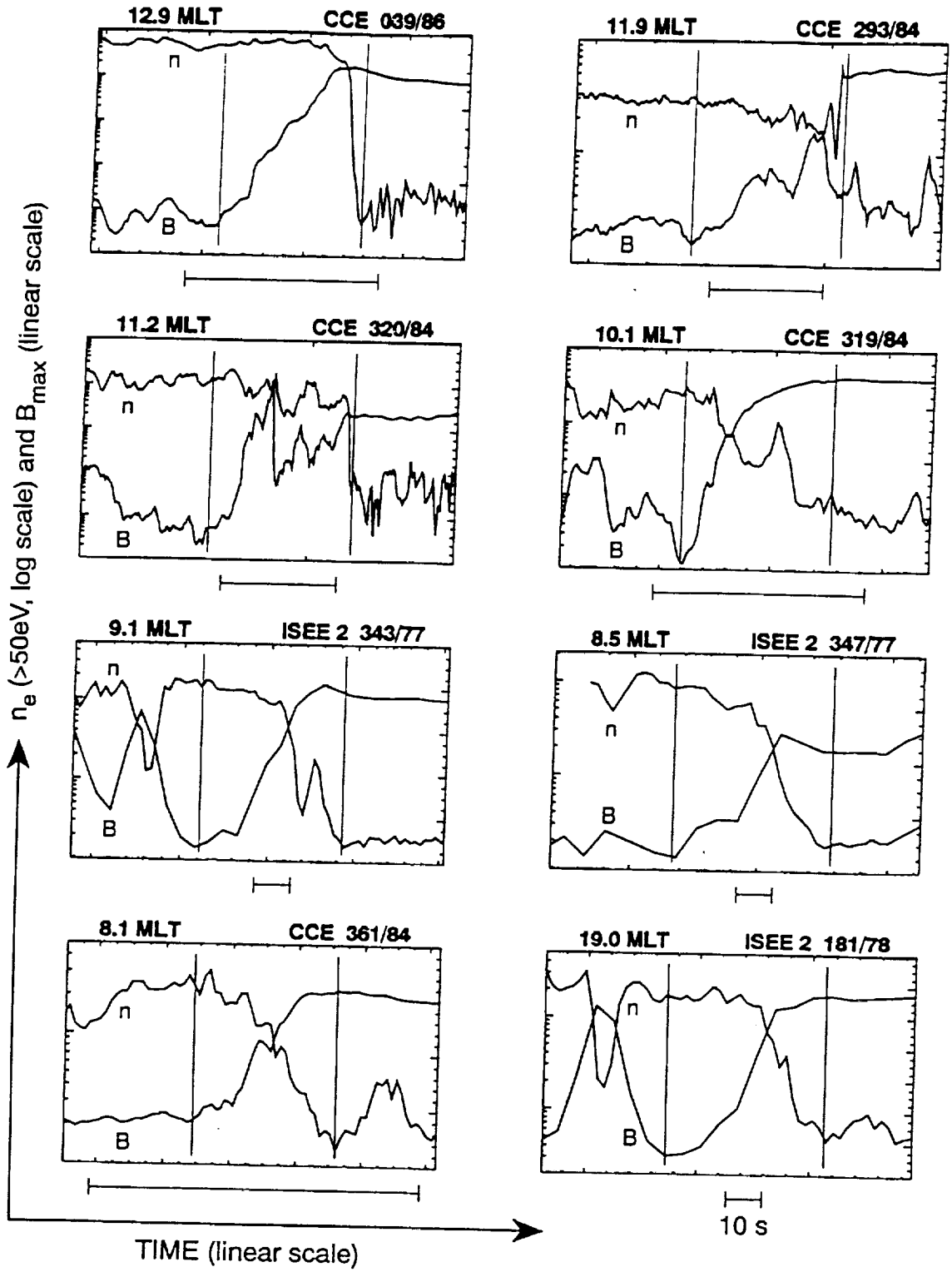

Figure 6. Local time dependence of magnetopause microstructure is illustrated by these eight CCE and ISEE 2 crossings at locations near noon to the dawn-dusk meridian. The magnetopause width is adjusted to be the same on each plot for easy comparison of the basic density (n) vs. field (B) structure (vertical scales are relative and a 10–sec baseline is given for each crossing).

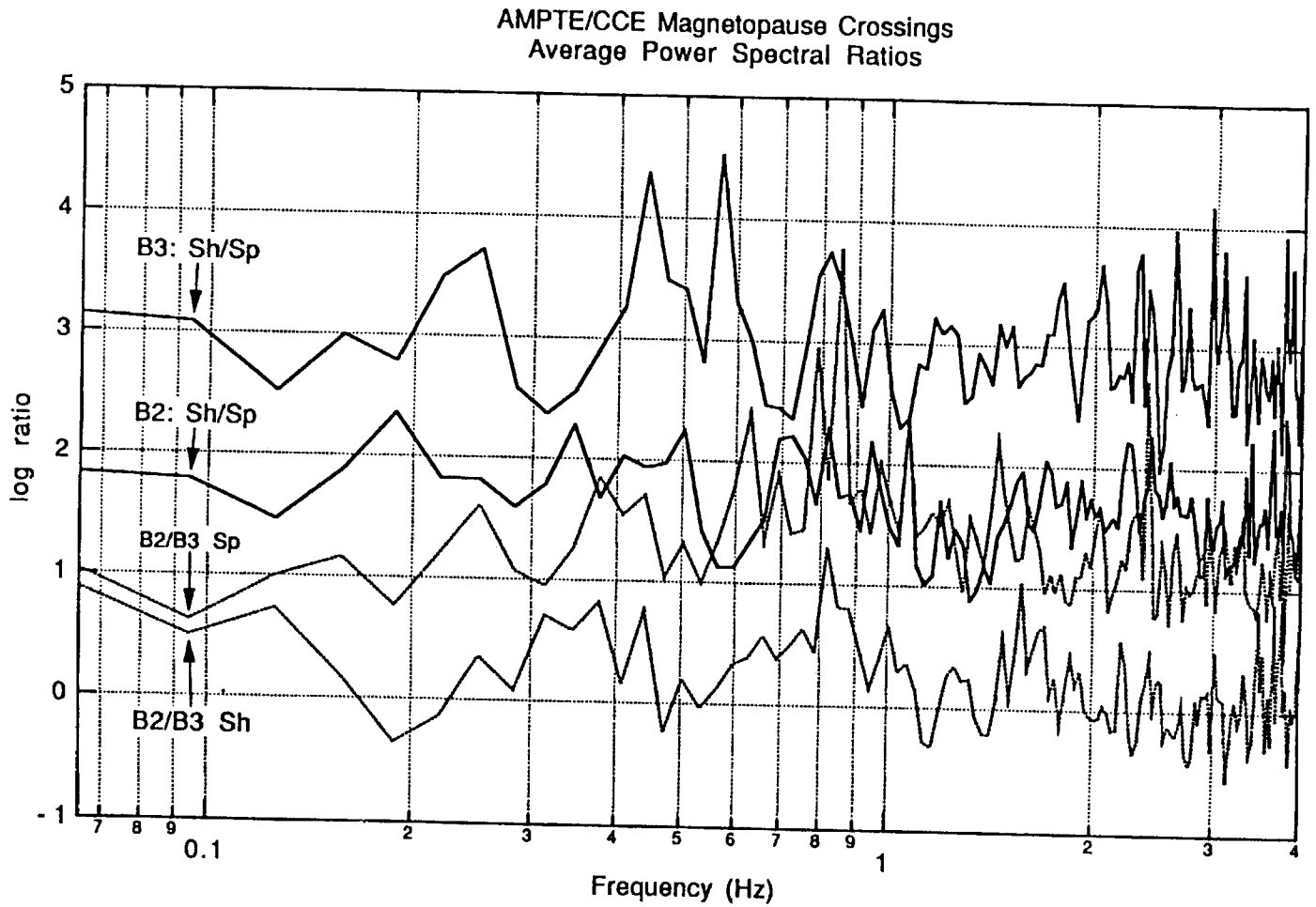

Figure 7. Average power spectral ratios are shown here based on CCE magnetometer observations near the magnetopause and averaged over all 10 cases analyzed. "Sh" and "Sp" denote adjoining intervals of magnetosheath and magnetosphere, respectively, and B2 and B3 denote intermediate and minimum variance components, respectively.

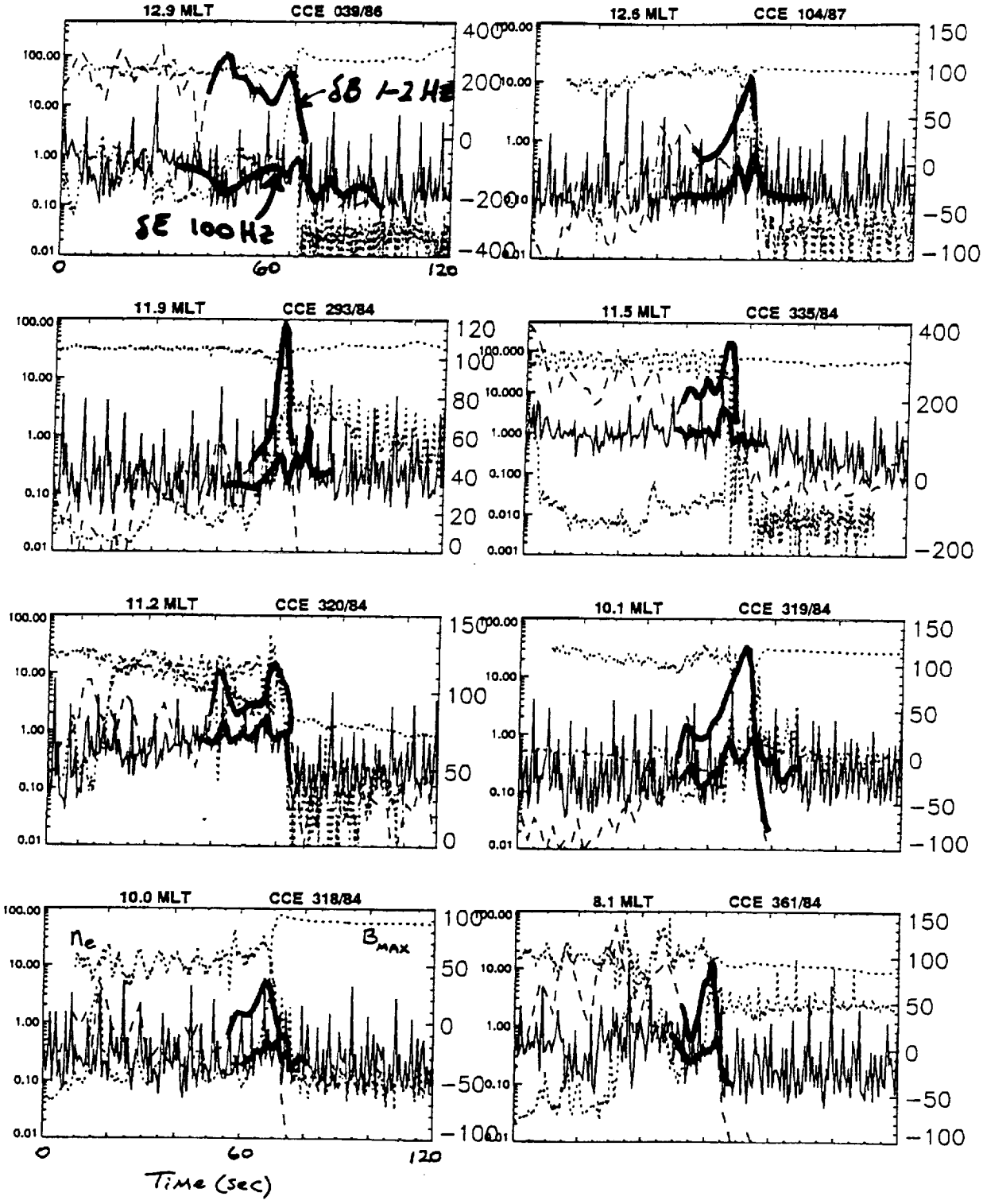

Figure 8. Observations from the CCE plasma wave experiment (PWE) are shown (courtesy of Dr. Robert Strangeway, UCLA). Electric (δE) and magnetic (δB) fluctuation levels are plotted for the 100 Hz electric and 1–2 Hz magnetic channels.

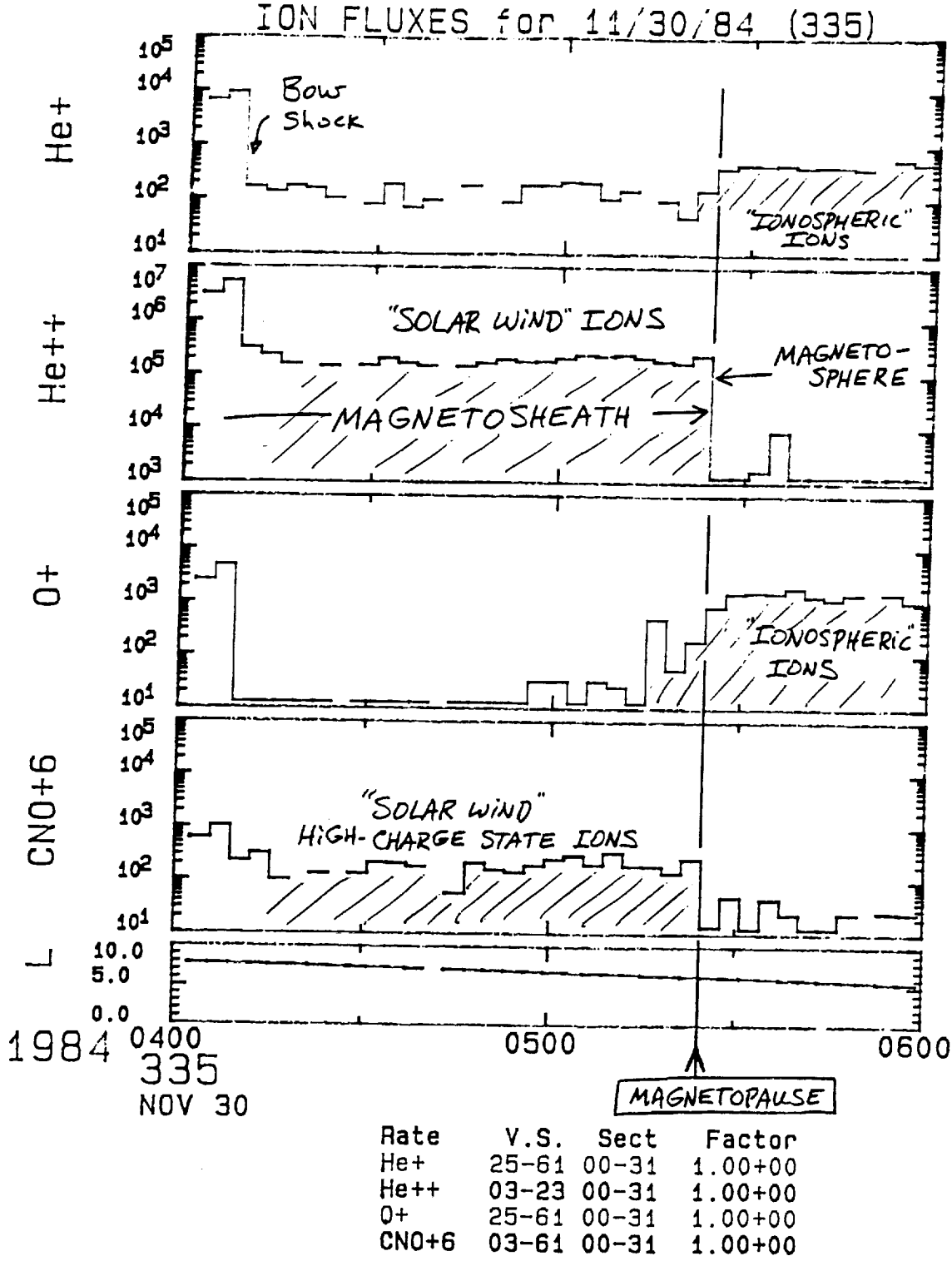

Figure 9. Fluxes for various ion species are plotted here for one CCE crossings based on the Charge-Energy-Mass (CHEM) experiment. Both the magnetopause and bow shock are marked along with basic ion "tracers;" note the "leakage" of ionospheric ions into the nearby magnetosheath.